Published in final edited form as:
Mol Cancer Ther. 2013 August ; 12(8): 1545–1555. doi:10.1158/1535-7163.MCT-12-0933.

Comparing Histone Deacetylase Inhibitor Responses in Genetically Engineered Mouse Lung Cancer Models and a Window of Opportunity Trial in Lung Cancer Patients

Tian Ma[1,*], **Fabrizio Galimberti**[1,*], **Cherie P. Erkmen**[2], **Vincent Memoli**[3,5], **Fadzai Chinyengetere**[1], **Lorenzo Sempere**[4], **Jan H. Beumer**[6,7], **Bean N. Anyang**[6], **William Nugent**[2], **David Johnstone**[2], **Gregory J. Tsongalis**[3], **Jonathan M. Kurie**[8], **Hua Li**[1], **James DiRenzo**[1,5], **Yongli Guo**[1], **Sarah J. Freemantle**[1], **Konstantin H. Dragnev**[4,5], and **Ethan Dmitrovsky**[1,4,5]

[1]Department of Pharmacology and Toxicology, Geisel School of Medicine at Dartmouth, Hanover, NH 03755

[2]Department of Surgery, Geisel School of Medicine at Dartmouth, Hanover, NH 03755

[3]Department of Pathology, Geisel School of Medicine at Dartmouth, Hanover, NH 03755

[4]Department of Medicine, Geisel School of Medicine at Dartmouth, Hanover, NH 03755

[5]Norris Cotton Cancer Center, Geisel School of Medicine at Dartmouth, Hanover, NH 03755 and Dartmouth-Hitchcock Medical Center, Lebanon, NH 03756

[6]Molecular Therapeutics/Drug Discovery Program, University of Pittsburgh Cancer Institute, Pittsburgh, PA 15213

[7]Department of Pharmaceutical Sciences, University of Pittsburgh School of Pharmacy, Pittsburgh, PA 15213

[8]MD Anderson Cancer Center, Houston, TX 77030

Abstract

Histone deacetylase inhibitor (HDACi, vorinostat) responses were studied in murine and human lung cancer cell lines and genetically-engineered mouse lung cancer models. Findings were compared with a window of opportunity trial in aerodigestive tract cancers. In human (HOP62, H522 and H23) and murine transgenic (ED-1, ED-2, LKR-13, and 393P, driven respectively by cyclin E, degradation-resistant cyclin E, KRAS, or KRAS/p53) lung cancer cell lines vorinostat reduced growth, cyclin D1 and cyclin E levels, but induced p27, histone acetylation and apoptosis. Other biomarkers also changed. Findings from transgenic murine lung cancer models were integrated with those from a window of opportunity trial that measured vorinostat pharmacodynamic responses in pre- versus post-treatment tumor biopsies. Vorinostat repressed cyclin D1 and cyclin E expression in murine transgenic lung cancers and significantly reduced lung cancers in syngeneic mice. Vorinostat also reduced cyclin D1 and cyclin E expression, but increased p27 levels in post- versus pre-treatment human lung cancer biopsies. Notably, necrotic and inflammatory responses appeared in post-treatment biopsies. These depended on intratumoral HDACi levels. Therefore, HDACi treatments of murine genetically-engineered lung cancer models exert similar responses (growth inhibition and changes in gene expression) as observed in

Address correspondence to: Ethan Dmitrovsky, M.D., Department of Pharmacology and Toxicology, Geisel School of Medicine at Dartmouth, Hanover, NH 03755. Phone: 603-650-1707; Fax: 603-650-1129. ethan.dmitrovsky@dartmouth.edu.
*These authors contributed equally to this manuscript.

Disclosure of Potential Conflicts of interest: Ethan Dmitrovsky, M.D. and Konstantin H. Dragnev, M.D. received research funding from Merck.

lung cancer cell lines. Moreover, enhanced pharmacodynamic responses occurred in the window of opportunity trial, providing additional markers of response that can be evaluated in subsequent HDACi trials. Thus, combining murine and human HDACi trials is a strategy to translate preclinical HDACi treatment outcomes into the clinic. This study uncovered clinically-tractable mechanisms to engage in future HDACi trials.

Keywords

histone deacetylase inhibitor; cyclins; lung cancer; window of opportunity trial

Introduction

Lung cancer is the leading cause of cancer-related death (1,2). Innovative ways to combat lung cancer are needed. Cell cycle deregulation contributes to uncontrolled growth of lung cancer. D-type and E-type cyclins regulate the G1-S transition; these cyclins are aberrantly expressed in lung carcinogenesis (3,4). Aberrant cyclin expression profiles have a negative prognosis in lung cancer (5–7). Induced changes in cyclin D1 or cyclin E expression are associated with responses to antineoplastic agents in lung cancer, as our group and others reported (8–15).

Human surfactant C-driven wild-type or proteasomal degradation-resistant cyclin E transgenic mice were engineered. These are tools for lung cancer biology and therapy studies since these mice recapitulate human lung cancer features (16,17). Lung cancer cell lines were independently derived from these genetically-engineered mice (18). After tail vein transplantation of these cells into syngeneic mice, lung cancers form; this permits testing of drugs that treat lung cancers (18–21). These and other engineered mouse lung cancer models were previously used to study antineoplastic effects of drugs that target cyclin E or cyclin D1 for repression (14,19,21).

Prior work was built upon by studying the histone deacetylase inhibitor (HDACi) vorinostat (suberoylanilide hydroxamic acid, SAHA or Zolinza). Vorinostat inhibits class I, II, and IV, but not class III HDACs, as reviewed (22–25). Histone deacetylases (HDACs) remove acetyl groups from histones, leading to chromatin condensation and transcriptional repression (22–25). HDAC knock-down causes check point arrest that inhibits cancer cell growth (26). Vorinostat targets the HDAC catalytic domain; this reduces growth of diverse cancer cell lines (including lung cancer cells) by cell cycle arrest via changes in expression of growth regulatory proteins (22–25,27,28).

Based on these pre-clinical HDACi activities, vorinostat clinical trials were conducted in advanced non-small cell lung cancer (NSCLC). Anti-tumor activity was modest for vorinostat treatment alone in relapsed NSCLCs (29,30). Activity increased when vorinostat was combined with chemotherapy (31,32). These findings implied that vorinostat effects in pre-clinical lung cancer models might not be recapitulated in tumors of vorinostat-treated lung cancer patients. This study sought to address this gap in knowledge of vorinostat anti-neoplastic actions.

This was accomplished by determining vorinostat pharmacodynamics in human lung cancer cell lines and in murine transgenic lung cancer cell lines engineered with genetic changes present in clinical lung cancers. Vorinostat anti-neoplastic responses were also studied in genetically-engineered mouse models that mimicked features of human lung cancer. Findings were compared to those found in a window of opportunity trial in previously untreated lung and esophageal cancer patients. Both pre- and post-vorinostat treatment tumor biopsies were obtained; serum and intratumoral vorinostat levels were measured.

These findings establish the value of translating results from vorinostat treatment of lung cancer cell lines into genetically-engineered mouse lung cancer models. Comparing responses to vorinostat treatment outcomes in lung cancer patients can uncover clinically-tractable pharmacodynamic mechanisms. These pathways could be engaged in future HDACi trials.

Materials and Methods

Cell culture treatments

Murine lung cancer cell lines from lung cancers of wild-type (ED-1) or proteasome degradation-resistant cyclin E (ED-2) transgenic mice exist (17,18). The 393P lung cancer cell line was from *Kras*$^{LA1/+}$; p53$^{R172H\Delta G/+}$ and the LKR-13 cell line was from *Kras*$^{LA2/WT}$ transgenic mice, respectively (33,34). Murine (ED-1, ED-2, 393P, and LKR-13) and human (HOP62, H522 and H23) lung cancer cell lines were cultured in RPMI-1640 media with 10% FBS and 1% antibiotic and antimycotic solution at 37°C with 5% CO_2 in a humidified incubator. Human lung cancer cell lines were obtained from and authenticated by the American Type Culture Collection and the murine lung cancer cell lines were previously authenticated (14,18). All lines tested negative for mycoplasma and were passaged less than 6 months after receipt or resuscitation. Vorinostat (Supplemental Fig. 1) was obtained from Dr. Jason Sparkowski (Merck, Whitehouse Station, NJ).

Logarithmically-growing lung cancer cells were seeded at optimized densities in six-well tissue culture plates. Proliferation and apoptosis assays were performed in triplicate and replicated at least three times. Cells were treated 24 hours later with vorinostat at varying concentrations versus vehicle (dimethyl sulfoxide, DMSO) controls and assayed at different times using the CellTiter-Glo kit (Promega, Madison, WI), as before (35). Apoptosis assays were performed with the Annexin V:FITC Kit (AbD Serotec, Raleigh, NC) in triplicate with independent replicates, as before (35). Drug washout experiments were conducted.

Immunoblot analyses

Immunoblot assays were performed as in prior work (16,35). These assays were with antibodies recognizing cyclin D1 (M-20, Santa Cruz Biotechnology, Santa Cruz, CA), cyclin E (M-20, Santa Cruz Biotechnology), p27 (C-19, Santa Cruz Biotechnology), anti-acetyl-histone H3 (Millipore, Billerica, MA), or actin (C-11, Santa Cruz Biotechnology). Other antibodies recognized acetylated alpha-tubulin (6–11B-1, Sigma, St. Louis, MO), alpha-tubulin (DM1A, Millipore), Akt (9272, Cell Signaling, Danvers, MA), phospho-Akt (Ser473, D9E, Cell Signaling), Bax (N-20, Santa Cruz Biotechnology), Bcl-2 (D55G8, Cell Signaling; N-19, Santa Cruz Biotechnology), Bim (C34C5, Cell Signaling), E-cadherin (24E10, Cell Signaling), Chk1 (G-4, Santa Cruz Biotechnology), c-Raf (9422, Cell Signaling), Mcl-1 (D35A5, Cell Signaling), p21 (12D1, Cell Signaling; F-5, Santa Cruz Biotechnology), or phospho-histone H2AX (Ser139, 2577, Cell Signaling).

Transgenic experiments

Nine-month old female transgenic mice expressing wild-type human cyclin E and that developed neoplastic lung lesions were injected (intraperitoneal, ip) with vorinostat (100mg/kg) or with an equal volume of vehicle (DMSO) daily for 5 days before being euthanized using an Institutional Animal Care and Use Committee (IACUC)-approved protocol. Lung tissues were harvested, formalin-fixed and paraffin-embedded, processed and sectioned for histopathology and hematoxylin and eosin (H & E) staining, or immunostaining as before (14,16). Quantification was by a pathologist (VM) unaware of treatment arm identities, as described (14,16). Three mice were used in each study arm.

In vivo tumorigenicity

Eight-week old female FVB mice were each tail vein injected with 8×10^5 early passage ED-1 cells suspended in phosphate buffered saline (PBS) with 10% mouse serum (Invitrogen, Carlsbad, CA). Lung tumors formed by 14 days (18–20) when mice were each injected with vorinostat (200mg/kg ip, 13 mice) dissolved in vehicle (10% DMSO, 45% PEG400 and 45% sterile water) or with an equal volume of vehicle (12 mice) for 14 consecutive days. Mice were euthanized using an IACUC-approved protocol. Lung tissues were harvested and processed with lung tumors scored by a pathologist (H.L.) blinded as to treatment arm identities.

Patients

Patients with clinical stage I, II, IIIA NSCLC or stage I esophageal cancer and a pre-treatment biopsy having at least 5 unstained slides were eligible. Inclusion criteria were adequate hepatic (hepatic transaminases ≤ 2.0 and total bilirubin ≤ 1.5 times the upper limit of normal) and renal (serum creatinine < 1.5 times the upper limit of normal and creatinine clearance ≥ 60mL/min) functions. Exclusion criteria were prior chemotherapy or radiotherapy, age < 18, serious uncontrolled comorbidities, active infection, inability to give informed consent because of altered mental status or cognitive impairment, prior use of HDACis, hypersensitivity to vorinostat or capsule components, concurrent use of other antineoplastics (approved or investigational) within 30 days of this study or use of valproic acid unless its use was not as an antineoplastic and a 30-day washout period occurred. Patients with a history of pulmonary embolism and not receiving anticoagulation were excluded.

Inclusion and exclusion criteria were assessed within 14 days before therapy began except for radiographic studies that were within 28 days of screening. Effective contraception or sexual abstinence was required for female patients of childbearing potential or male patients with female partners of childbearing potential. This trial was conducted after review and approval by the Committee for the Protection of Human Subjects at Dartmouth College and the Institutional Review Board. Informed consent was obtained from patients before their enrollment onto this trial that was registered on the clinicaltrials.gov website as NCT00735826.

Study drugs

Subjects received oral administration of the established phase II dosage (29) of vorinostat 400mg once daily for up to 9 days before surgical resection and on the day of surgery.

Clinical trial endpoints

Prespecified response endpoints for the window of opportunity trial were a 50% decrease in cyclin D1 or cyclin E immunohistochemical expression (post- versus pre-treatment biopsies) and tumor vorinostat concentrations. The prespecified number of evaluable cases for the window of opportunity trial was 10. If only one or fewer than 10 patients responded, the study would exclude response rates of 25.6% or higher with $P < 0.05$ (36). Significance was defined as $P < 0.05$.

Pharmacokinetics

Subjects took vorinostat in mornings with food and fasting on the day of biopsy/surgery. The dose on the day of biopsy/surgery was taken under medical supervision and its time recorded. Serum samples were obtained before vorinostat treatment and at the time of biopsy. Serum was isolated by centrifugation at 0°C and at 1500 × g for 10 min before storage at −70 °C. Biopsied tumors were immediately snap-frozen in liquid nitrogen and

stored at −70 °C until analysis. Tumor tissue was homogenized in 3 parts PBS (1:3; g/v). Vorinostat was quantitated using an established FDA-validated LC-MS/MS assay (37). Tumor homogenates were processed as serum and quantitated against a serum calibration curve. Analysis of quality control samples prepared in control human lung tumor homogenate proved that tumor homogenate could be processed as serum. Vorinostat was accurately quantitated against a serum calibration curve.

Tissue analyses

One portion of a tumor was harvested at resection, formalin-fixed and processed for histopathology and immunostaining, as before (14,16). Another portion was immediately snap-frozen in liquid nitrogen for vorinostat pharmacodynamics and pharmacokinetics. Immunostaining for cyclin D1, cyclin E, Ki-67, caspase, p27, p21 and other markers were performed by a pathologist (V.M.), who used optimized assays (15,16,19). The scoring system used for immunostaining and inflammatory infiltrates was previously described (14). Fluorescence-based multiplex assays (38) were with a staining station (Leica Microsystems, Buffalo Grove, IL) using antibodies to detect T cells with CD8 (Leica), macrophages with CD68 (Leica), B cells with CD20 (Leica), or myeloid cells with myeloperoxidase (MPO, Thermo Fisher Scientific, Waltham, MA).

EGFR and KRAS mutational analyses

Genomic DNA was isolated from paraffin-embedded sections from study cases and independently analyzed for *EGFR* and *KRAS* mutations using optimized methods (14).

Statistical analyses

Two-tailed t tests were used for statistical analyses. The Welch modified two-sample t-test was also used for statistical analyses of the mouse tumor experiments.

Results

Vorinostat effects in transgenic lung cancer cells

Vorinostat effects on proliferation, apoptosis, histone acetylation and cell cycle regulatory proteins were studied because prior work implicated these and other changes as important for HDACi responses (22–25). Genetically-defined murine transgenic lung cancer cell lines were studied because they recapitulated features of human lung cancers (17,18,33,34). These lines deregulated cyclin E (ED-1 and ED-2), or had *KRAS* (LKR-13) or *KRAS* and *p53* (393P) mutations. Fig. 1A and 1B established dose- and time-dependent effects on growth and apoptosis in ED-1 and ED-2 cells. Growth inhibition was reversible after drug washouts (Fig. 1C). Acetylation and p27 levels increased, but cyclin D1 and cyclin E expression decreased in ED-1 cells (Fig. 1D), a representative murine lung cancer line. Vorinostat activities were also examined in LKR-13 and 393P murine transgenic lung cancer cell lines in Fig. 2. These exhibited similar, but less prominent vorinostat treatment effects than did ED-1 or ED-2 cells.

Vorinostat effects in human lung cancer cell lines

Vorinostat effects were investigated in HOP62, H522 and H23 human lung cancer cell lines. Similar to findings in murine lung cancer cells, vorinostat significantly reduced growth of each of these lines in a dose- and time-dependent manner (Fig. 3A). Vorinostat-mediated changes in apoptosis were confirmed in HOP62, a representative human lung cancer line (Fig 3B). Vorinostat growth inhibition was reversed by drug washout (Fig. 3C). Vorinostat exhibited dose-dependent effects on acetylation and cell cycle regulatory proteins (Fig. 3D). Therefore, vorinostat exhibited substantial anti-neoplastic effects in murine and human lung

cancer cells at clinically achievable concentrations (31). Other biomarkers of HDACi response were compared in murine and human lung cancer cells lines in Supplemental Fig. 2. These studies revealed that specific Bcl-2 family members and other species were regulated by vorinostat treatments of these lung cancer cells. These findings were extended by showing that c-Raf and phospho-AKT levels declined, but p21, acetylated tubulin, and expression of the epithelial-mesenchymal transition (EMT) marker E-cadherin increased after vorinostat treatments (Supplemental Fig. 2).

Vorinostat effects in murine transgenic models

To explore *in vivo* vorinostat treatment effects, studies were independently performed using murine syngeneic transplantable and transgenic cyclin E-driven lung cancer models. Two weeks after tail vein injections of ED-1 cells, FVB mice were treated with vorinostat (200mg/kg) or an equal volume of vehicle as a control by daily ip injections for 14 days. Lung cancers were scored as before (19). Figs. 4A and 4B revealed that vorinostat significantly reduced the number of lung cancers in mice versus controls.

To evaluate pharmacodynamic effects, transgenic cyclin E mice that spontaneously developed lung cancer were injected with vorinostat (100mg/kg/ip) or an equal volume of vehicle for 5 consecutive days. Results in Fig. 4C revealed a substantial decline in cyclin D1 and cyclin E expression in these lung cancers by vorinostat versus control treatments. There were no appreciable changes in Ki-67, caspase, and p27 levels in these tumors; inflammation and necrosis were not observed in treated tumors (data not shown). Whether changes in these endpoints occurred in tumors during vorinostat treatments of cancer patients were next studied.

Patient characteristics and vorinostat clinical responses

Fifteen early stage lung or esophageal cancer patients were enrolled between July 23, 2009 and August 23, 2011 onto a vorinostat window of opportunity trial. Ten received two or more days of treatment and had sufficient paired pre-versus post-treatment tumors for histopathologic, pharmacodynamic, and pharmacokinetic studies. Clinical, histopathologic, pharmacodynamic and pharmacokinetic findings appear in Table 1. Median age was 67 years with 4 women (40%) and 6 men (60%). One (10%) patient had squamous cell cancer (SCC) of the lung, 6 (60%) had lung (ADC) or esophageal (Eso-ADC) adenocarcinomas, and 3 (30%) had adenocarcinomas with bronchioloalveaolar (BAC) features. Five (50%) patients were former or never smokers; five (50%) were current smokers.

All cases had wild-type epidermal growth factor receptor (EGFR, data not shown) sequences; 4 had *KRAS* codon 12 mutations in their lung cancers (Table 1). Seven cases (70%) reduced Ki-67 expression in post- versus pre-treatment tumors. Cyclin E and/or cyclin D1 immunohistochemical expression decreased in 4 (40%) post-treatment tumors. Caspase levels were at the limits of detection. Induction of p27 occurred in a representative post- versus pre-treatment lung cancer (Fig. 5A). Increased p21 tumor expression was also observed after vorinostat treatment (Supplemental Fig. 3). There were insufficient biopsies to analyze HDACi biomarkers shown in Supplemental Fig. 2.

Intriguingly, 8 (80%) of post-treatment, but not pre-treatment tumors exhibited substantial necrosis and/or acute or chronic inflammation (Table 1). Multiplex immunohistochemical assays were used to identify cells expressing CD8, CD68, CD20, or MPO markers that respectively detected cytotoxic T cells, macrophages, B cells, or neutrophils. CD68+ and MPO+ cells with increased numbers of CD20+ and CD8+ cells appeared in post-treatment tumors (Fig. 5B), consistent with inflammatory responses.

These responses were correlated with presence of *KRAS* mutations in these tumors (Table 1). Esophageal cancer cases were eligible for this trial to assess vorinostat treatment effects beyond lung cancers. All 4 NSCLC cases with *KRAS* mutations had necrosis, and acute or chronic inflammation in post-treatment tumors. These post-treatment tumors had a decline in K-67 expression, 2 had a decrease in cyclin E, and 1 case had a decrease in cyclin D1 expression. Thus, responses were independent of *KRAS* mutations in tumors (Table 1).

Vorinostat pharmacokinetics

Vorinostat levels in resected tumors were quantitated in evaluable patients. Pharmacokinetic analyses confirmed serum and tumor concentrations above the detection limits of the assay in 8 (80%) and 7 (70%) patients, respectively. One other patient took vorinostat for only 3 days with surgery performed 4 days later; the other patient took the study drug at 25% of the dose (100 mg) for 7 days, indicating that reduced dose or duration of treatment decreased vorinostat concentrations. There was interindividual variation in serum vorinostat concentrations (range, 7.3–192.4 ng/ml; coefficient of variation (CV) 95%) and intratumoral levels (range, 15.0–80.3 ng/g; CV 59%). The highest intratumoral drug level (34024 ng/g) was in the esophageal cancer case, likely from contaminating vorinostat in the mucosa. Lung tumor concentrations detected were similar to those observed in patient-matched serum. This is consistent with the reported volume of distribution of approximately 60–100 L/m^2, close to 1 L/kg (39). The relationship between vorinostat pharmacodynamics and intratumoral vorinostat measurements is presented in Table 1. Changes in multiple biomarkers were observed across the range of tumor vorinostat levels (range, 15.0 – 34024 ng/g).

Discussion

The study compared responses to the HDACi vorinostat in genetically-engineered mouse models that mimic clinical lung cancers with results from a window of opportunity trial in lung cancer patients. Figs. 1 and 2 and Supplemental Fig. 2 revealed that murine transgenic lung cancer cell lines responded to this HDACi with dose-and time-dependent growth inhibition, increased apoptosis and histone acetylation and changes in expressed cell cycle regulators: p27, cyclin D1, cyclin E and other vorinostat biomarkers. Human lung cancer cell lines exhibited similar effects (Fig. 3 and Supplemental Fig. 2). Notably, vorinostat reduced lung cancer formation in a murine syngeneic transplantation model and decreased cyclin D1 and cyclin E expression in transgenic lung cancers (Fig. 4). Thus, prior work (40) was extended by showing that vorinostat induced similar changes in expressed cell cycle regulatory proteins *in vitro* and *in vivo*. Vorinostat chemopreventive effects in murine carcinogen-induced lung tumors (41) were confirmed and extended here using a transplantable lung cancer model (Fig. 4).

Clinical implications of this work were explored in a vorinosat window of opportunity trial. Pharmacodynamic responses in Fig. 5 and Table 1 included changes in expressed cell cycle regulators and reduced proliferation of human tumors despite the presence of *KRAS* mutations. Treatment of *KRAS* harboring lung cancer cases is an unmet clinical need (14). Intriguingly, vorinostat induced inflammation and necrosis in post-treatment tumors. Combining an agent that engages necrotic or inflammatory responses might augment clinical activity of vorinostat or another HDACi.

Differences between murine and human lung cancer responses to this HDACi could relate to the timing of post-treatment biopsies. For example, increased p27 levels and apoptosis were early indicators of vorinostat responses in cultured lung cancer cells (Figs. 1–3). Yet, the post-treatment biopsies in Table 1 were obtained at later time points. The presence of necrosis in the post-treatment human tumors implied that a wave of apoptosis and

inflammation preceded the onset of necrosis. These findings indicate the value of integrating results from genetically-engineered mouse models with those from a mechanistic clinical trial. This co-clinical trial approach extends prior work (42,43).

Both serum and intratumoral vorinostat concentrations were measured in this clinical trial. This made possible comparisons of intratumoral pharmacodynamics and pharmacokinetics. Comparable drug concentrations were needed in *in vitro* models and in clinical tumors to achieve pharmacodynamic responses. Intratumoral drug levels depended on the vorinostat dose and on the timing of the post-treatment biopsy relative to the last vorinostat dosage. An esophageal cancer case had the highest vorinostat level. This was likely from the presence of vorinostat after an oral dosage. Tumor-specific expression or activity of drug transporters might also contribute to changes in vorinostat levels (44). Future work should consider these possibilities and whether clinical toxicity or resistance (22–24,44) is reduced by the HDACi dose schedule.

Vorinostat was administered to lung cancer patients as a single agent or as a combination regimen (29–32). Clinical activity against lung cancers increased when vorinostat was combined with chemotherapy (31,32). This prior work indicated a need to determine vorinostat pharmacodynamics in clinical lung cancers. This was addressed in this study by determining vorinostat intratumoral pharmacodynamics and pharmacokinetics in treated human lung cancers. Vorinostat exerted substantial antineoplastic effects in these cancers, including previously unrecognized ones: induced inflammation and necrosis. There is also a need to understand the basis for differences between the current and prior (29–32) vorinostat lung cancer trials.

Several explanations could account for these differences. Clinical vorinostat responses might differ in chemotherapy-resistant versus untreated cancer cases as accrued to the window of opportunity trial. Vorinostat resistance could develop after prolonged treatments (22,24,44). Vorinostat can induce expression of drug resistance-associated ABC transporters in tumors (44,45). Also, p21 is involved in drug resistance and vorinostat can augment p21 expression (46,47). After p21 knockdown, cancer cells become sensitive to vorinostat treatment (47).

Interestingly, p21 immunohistochemical expression increased in a representative post-vorinostat versus pre-treatment lung cancer (Supplemental Fig. 3). This tumor might exhibit vorinostat resistance. Consistent with this is the finding that temisirolimus decreased p21 expression (without affecting cyclin D1 expression); this enhanced vorinostat anti-neoplastic effects in mantle cell lymphoma (47). Future cancer trials should consider using combination regimens and schedules that limit onset of vorinostat resistance. Proof of concept could be established using genetically-engineered lung cancer models described here or with xenograft lung cancer models. Given the observed pharmacodynamic effects on cyclin D1 and cyclin E levels in murine and human lung cancers, combination vorinostat regimens are appealing that would repress these cyclins and blunt increased p21 expression. There is also a rationale for a regimen that combines an HDACi with a DNA damaging agent (48).

In summary, substantial anti-neoplastic effects were observed for the HDACi vorinostat in murine and human lung cancer cell lines as well as in murine transgenic and transplantation lung cancer models. Findings were translated into a vorinostat window of opportunity clinical trial where induced p21 and p27 and reduced G1 cyclin expression occurred in lung cancers independent of the presence of *KRAS* mutations. These anti-tumor responses were accompanied by inflammatory and necrotic changes in human tumors.

Whether vorinostat anti-neoplastic activities against human tumors reported here will translate into a survival advantage is the subject of future work. Vorinostat alone may not

suffice in treating lung or esophageal cancers. Yet, combining vorinostat with surgery or radiation therapy and agents that reduce cyclin D1 or blunt p21 expression could augment vorinostat therapeutic activity. Intermittent vorinostat treatments might reduce its toxicity or resistance. Genetically-engineered lung cancer models described here are useful to design future vorinostat trials.

Supplementary Material

Refer to Web version on PubMed Central for supplementary material.

Acknowledgments

We thank Dr. Jason Sparkowski (Merck) for providing us vorinostat. We thank Dr. Eugene Demidenko, Department of Community and Family Medicine at Geisel School of Medicine at Dartmouth for biostatistical consultation and Drs. Alan Eastman, Alexey Danilov, Yolanda Sanchez, and Michael Sporn (Geisel School of Medicine) for providing several antibodies.

Grant Support

This study was supported by National Institutes of Health (NIH) and National Cancer Institute (NCI) grants R01-CA087546 (E. Dmitrovsky and S.J. Freemantle), R01-CA111422 (E. Dmitrovsky and S.J. Freemantle), and U01-CA099168 (J.H. Beumer), by a Samuel Waxman Cancer Research Foundation award (E. Dmitrovsky), by a grant from Merck (K.H. Dragnev., E. Dmitrovsky) and by an American Cancer Society Clinical Research Professorship (E. Dmitrovsky) provided by a generous gift from the FM Kirby Foundation. This project used the UPCI Clinical Pharmacology Analytical Facility (CPAF) and was supported partly by NIH award P30CA047904 (J.H. Beumer, B.N. Anyang). Dartmouth's Norris Cotton Cancer Center Shared Resources were used and supported by NCI Core Grant 5P30CA023108.

Abbreviations

HDAC	Histone deacetylase
HDACi	histone deacetylase inhibitor
NSCLC	non-small cell lung cancer
ip	intraperitoneal
DMSO	dimethyl sulfoxide
H & E	hematoxylin and eosin
EGFR	epidermal growth factor receptor
IACUC	Institutional Animal Care and Use Committee
EMT	epithelial-mesenchymal transition

References

1. Siegel R, Ward E, Brawley O, Jemal A. Cancer statistics, 2011: the impact of eliminating socioeconomic and racial disparity on premature deaths. CA Cancer J Clin. 2011; 61:212–36. [PubMed: 21685461]
2. Garcia, M.; Jemal, A.; Ward, E.; Center, MM.; Hao, Y.; Siegel, RL., et al. Global cancer facts & figures 2007. Atlanta, GA: American Cancer Society; 2007.
3. Lonardo F, Rusch V, Langenfeld J, Dmitrovsky E, Klimstra DS. Overexpression of cyclins D1 and E is frequent in bronchial preneoplasia and precedes squamous cell carcinoma development. Cancer Res. 1999; 59:2470–6. [PubMed: 10344760]
4. Ratschiller D, Heighway J, Gugger M, Kappeler A, Pirnia F, Schmid RA, et al. Cyclin D1 overexpression in bronchial epithelia of patients with lung cancer is associated with smoking and predicts survival. J Clin Oncol. 2003; 21:2085–93. [PubMed: 12775733]

5. Betticher DC, Heighway J, Hasleton PS, Altermatt HJ, Ryder WD, Cerny T, et al. Prognostic significance of CCND1 (cyclin D1) overexpression in primary resected non-small-cell lung cancer. Br J Cancer. 1996; 73:294–300. [PubMed: 8562333]
6. Fukuse T, Hirata T, Naiki H, Hitomi S, Wada H. Prognostic significance of cyclin E overexpression in resected non-small cell lung cancer. Cancer Res. 2000; 60:242–4. [PubMed: 10667567]
7. Mishina T, Dosaka-Akita H, Hommura F, Nishi M, Kojima T, Ogura S, et al. Cyclin E expression, a potential prognostic marker for non-small cell lung cancers. Clin Cancer Res. 2000; 6:11–6. [PubMed: 10656426]
8. Freemantle SJ, Liu X, Feng Q, Galimberti F, Blumen S, Sekula D, et al. Cyclin degradation for cancer therapy and chemoprevention. J Cell Biochem. 2007; 102:869–77. [PubMed: 17868090]
9. Dragnev KH, Pitha-Rowe I, Ma Y, Petty WJ, Sekula D, Murphy B, et al. Specific chemopreventive agents trigger proteasomal degradation of G1 cyclins: implications for combination therapy. Clin Cancer Res. 2004; 10:2570–7. [PubMed: 15073138]
10. Papadimitrakopoulou VA, Izzo J, Mao L, Keck J, Hamilton D, Shin DM, et al. Cyclin D1 and p16 alterations in advanced premalignant lesions of the upper aerodigestive tract: role in response to chemoprevention and cancer development. Clin Cancer Res. 2001; 7:3127–34. [PubMed: 11595705]
11. Boyle JO, Langenfeld J, Lonardo F, Sekula D, Reczek P, Rusch V, et al. Cyclin D1 proteolysis: a retinoid chemoprevention signal in normal, immortalized, and transformed human bronchial epithelial cells. J Natl Cancer Inst. 1999; 91:373–9. [PubMed: 10050872]
12. Langenfeld J, Kiyokawa H, Sekula D, Boyle J, Dmitrovsky E. Posttranslational regulation of cyclin D1 by retinoic acid: a chemoprevention mechanism. Proc Natl Acad Sci USA. 1997; 94:12070–4. [PubMed: 9342364]
13. Petty WJ, Dragnev KH, Memoli VA, Ma Y, Desai NB, Biddle A, et al. Epidermal growth factor receptor tyrosine kinase inhibition represses cyclin D1 in aerodigestive tract cancers. Clin Cancer Res. 2004; 10:7547–54. [PubMed: 15569985]
14. Dragnev KH, Ma T, Cyrus J, Galimberti F, Memoli V, Busch A, et al. Bexarotene plus erlotinib suppress lung carcinogenesis independent of *KRAS* mutations in two clinical trials and transgenic models. Cancer Prev Res. 2011; 4:818–28.
15. Dragnev KH, Petty WJ, Shah SJ, Lewis LD, Black CC, Memoli V, et al. A proof-of-principle clinical trial of bexarotene in patients with non-small cell lung cancer. Clin Cancer Res. 2007; 13:179–800.
16. Ma Y, Fiering S, Black C, Liu X, Yuan Z, Memoli VA, et al. Transgenic cyclin E triggers dysplasia and multiple pulmonary adenocarcinomas. Proc Natl Acad Sci USA. 2007; 104:4089–94. [PubMed: 17360482]
17. Freemantle SJ, Dmitrovsky E. Cyclin E transgenic mice: discovery tools for lung cancer biology, therapy and prevention. Cancer Prev Res. 2010; 3:1513–8.
18. Liu X, Sempere LF, Galimberti F, Freemantle SJ, Black C, Dragnev KH, et al. Uncovering growth-suppressive MicroRNAs in lung cancer. Clin Cancer Res. 2009; 15:1177–83. [PubMed: 19228723]
19. Galimberti F, Thompson SL, Liu X, Li H, Memoli V, Green SR, et al. Targeting the cyclin E-Cdk-2 complex represses lung cancer growth by triggering anaphase catastrophe. Clin Cancer Res. 2010; 16:109–20. [PubMed: 20028770]
20. Liu X, Sempere LF, Ouyang H, Memoli VA, Andrew AS, Luo Y, et al. MicroRNA-31 functions as an oncogenic microRNA in mouse and human lung cancer cells by repressing specific tumor suppressors. J Clin Invest. 2010; 120:1298–309. [PubMed: 20237410]
21. Galimberti F, Busch AM, Chinyengetere F, Ma T, Sekula D, Memoli V, et al. Response to smoothened inhibition in diverse epithelial cancers that lack smoothened or patched 1 mutations. Int J of Oncol. 2012; 41:1751–61. [PubMed: 22923130]
22. Marks PA. Discovery and development of SAHA as an anti-cancer agent. Oncogene. 2007; 26:1351–6. [PubMed: 17322921]
23. Xu WS, Parmigiani RB, Marks PA. Histone deacetylase inhibitors: molecular mechanisms of action. Oncogene. 2007; 26:5541–52. [PubMed: 17694093]

24. Lane AA, Chabner BA. Histone deacetylase inhibitors in cancer therapy. J Clin Oncol. 2009; 27:5459–68. [PubMed: 19826124]
25. Schrump DS. Cytotoxicity mediated by histone deacetylase inhibitors in cancer cells: mechanisms and potential clinical implications. Clin Cancer Res. 2009; 14:3947–57. [PubMed: 19509170]
26. Senese S, Zaragoza K, Minardi S, Muradore I, Ronzoni S, Passafaro A, et al. Role for histone deacetylase 1 in human tumor cell proliferation. Mol Cell Biol. 2007; 27:4784–95. [PubMed: 17470557]
27. Finnin MS, Donigian JR, Cohen A, Richon VM, Rifkind RA, Marks PA, et al. Structures of a histone deacetylase homologue bound to the TSA and SAHA inhibitors. Nature. 1999; 401:188–93. [PubMed: 10490031]
28. Miyanaga P, Gemma A, Noro R, Kataoka K, Matsuda K, Nara M, et al. Antitumor activity of histone deacetylase inhibitors in non-small cell lung cancer cells: development of a molecular predictive model. Mol Cancer Ther. 2008; 7:1923–30. [PubMed: 18606719]
29. Traynor AM, Dubey S, Eickhoff JC, Kolesar JM, Schell K, Huie MS, et al. Vorinostat (NSC# 701852) in patients with relapsed non-small cell lung cancer: a Wisconsin Oncology Network phase II study. J Thorac Oncol. 2009; 4:522–6. [PubMed: 19347984]
30. Vansteenkiste J, Van Cutsem E, Dumez H, Chen C, Ricker JL, Randolph SS, et al. Early phase II trial of oral vorinostat in relapsed or refractory breast, colorectal, or non-small cell lung cancer. Invest New Drugs. 2008; 26:483–8. [PubMed: 18425418]
31. Ramalingam SS, Parise RA, Ramanathan RK, Lagattuta TF, Musguire LA, Stoller RG, et al. Phase I and pharmacokinetic study of vorinostat, a histone deacetylase inhibitor in combination with carboplatin and paclitaxel for advanced solid malignancies. Clin Cancer Res. 2007; 13:3605–10. [PubMed: 17510206]
32. Ramalingam SS, Maitland ML, Frankel P, Argiris AE, Koczywas M, Gitlitz B, et al. Carboplatin and paclitaxel in combination with either vorinostat or placebo in first-line therapy of advanced non-small cell lung cancer. J Clin Oncol. 2010; 28:56–62. [PubMed: 19933908]
33. Gibbons DL, Lin W, Creighton CJ, Rizvi ZH, Gregory PA, Goodall GJ, et al. Contextual extracellular cues promote tumor cell EMT and metastasis by regulating miR-200 family expression. Genes Dev. 2009; 23:2140–51. [PubMed: 19759262]
34. Wislez M, Spencer ML, Izzo JG, Juroske DM, Balhara K, Cody KK, et al. Inhibition of mammalian target of rapamycin reverses alveolar epithelial neoplasia induced by oncogenic k-ras. Cancer Res. 2005; 65:3226–35. [PubMed: 15833854]
35. Guo Y, Dolinko AV, Chinyengetere F, Stanton B, Bomberger JM, Demidenko E, et al. Blockade of the ubiquitin protease UBP43 destabilizes transcription factor PML/RARα and inhibits the growth of acute promyelocytic leukemia. Cancer Res. 2010; 70:9875–85. [PubMed: 20935222]
36. Clopper C, Pearson ES. The use of confidence or fiducial limits illustrated in the case of the binomial. Biometrika. 1934; 26:404–13.
37. Parise RA, Holleran JL, Beumer JH, Ramalingam S, Egorin MJ. A liquid chromatography-electrospray ionization tandem mass spectrometric assay for quantitation of the histone deacetylase inhibitor, vorinostat (suberoylanilide hydroxamic acid, SAHA), and its metabolites in human serum. J Chromatogr B Analyt Technol Biomed Life Sci. 2006; 840:108–15.
38. Sempere LF, Preis M, Yezefski T, Ouyang H, Suriawinata AA, Silahtaroglu A, et al. Fluorescence-based codetection with protein markers reveals distinct cellular compartments for altered microRNA expression in solid tumors. Clin Cancer Res. 2010; 16:4246–55. [PubMed: 20682703]
39. Kelly WK, Richon VM, O'Connor O, Curley T, MacGregor-Curtelli B, Tong W, et al. Phase I clinical trial of histone deacetylase inhibitor: suberoylanilide hydroxamic acid administered intravenously. Clin Cancer Res. 2003; 9:3578–88. [PubMed: 14506144]
40. Komatsu N, Kawamata N, Takeuchi S, Yin D, Chien W, Miller CW, et al. SAHA, a HDAC inhibitor, has profound anti-growth activity against non-small cell lung cancer cells. Oncol Rep. 2006; 15:187–91. [PubMed: 16328054]
41. Desai D, Das A, Cohen L, el-Bayoumy K, Amin S. Chemopreventive efficacy of suberoylanilide hydroxamic acid (SAHA) against 4-(methylnitrosamino)-1-(3-pyridyl)-1-butanone (NNK)-induced lung tumorigenesis in female A/J mice. Anticancer Res. 2003; 23:499–503. [PubMed: 12680257]

42. Singh M, Murriel CL, Johnson L. Genetically engineered mouse models: Closing the gap between preclinical data and trial outcomes. Cancer Res. 2012; 72:2695–700. [PubMed: 22593194]
43. Chen Z, Cheng K, Walton Z, Wang Y, Ebi H, Shimamura T, et al. A murine lung cancer co-clinical trial identifies genetic modifiers of therapeutic response. Nature. 2012; 483:613–7. [PubMed: 22425996]
44. Robey RW, Chakraborty AR, Basseville A, Luchencko V, Bahr J, Zhan A, et al. Histone deacetylase inhibitors: emerging mechanisms of resistance. Mol Pharm. 2011; 6:2021–31. [PubMed: 21899343]
45. Hauswald S, Duque-Afonso J, Wagner MM, Schertl FM, Lübbert M, Peschel C, et al. Histone deacetylase inhibitors induce a very broad, pleiotropic anticancer drug resistance phenotype in acute myeloid leukemia cells by modulation of multiple ABC transporter genes. Clin Cancer Res. 2009; 15:3705–15. [PubMed: 19458058]
46. Vrana J, Decker R, Johnson C, Wang Z, Jarvis W, Richon V, et al. Induction of apoptosis in U937 human leukemia cells by suberoylanilide hydroxamic acid (SAHA) proceeds through pathways that are regulated by Bcl-2/Bcl-XL, c-Jun, and p21CIP1, but independent of p53. Oncogene. 1999; 18:7016–25. [PubMed: 10597302]
47. Yazbeck VY, Buglio D, Georgakis GV, Li Y, Iwado E, Romaguera JE, et al. Temsirolimus downregulates p21 without altering cyclin D1 expression and induces autophagy and synergizes with vorinostat in mantle cell lymphoma. Exp Hematol. 2008; 36:443–50. [PubMed: 18343280]
48. Luchenko VL, Salcido CD, Zhang Y, Agama K, Komlodi-Pasztor E, Murphy RF, et al. Schedule-dependent synergy of histone deacetylase inhibitors with DNA damaging agents in small cell lung cancer. Cell Cycle. 2011; 10:3119–28. [PubMed: 21900747]

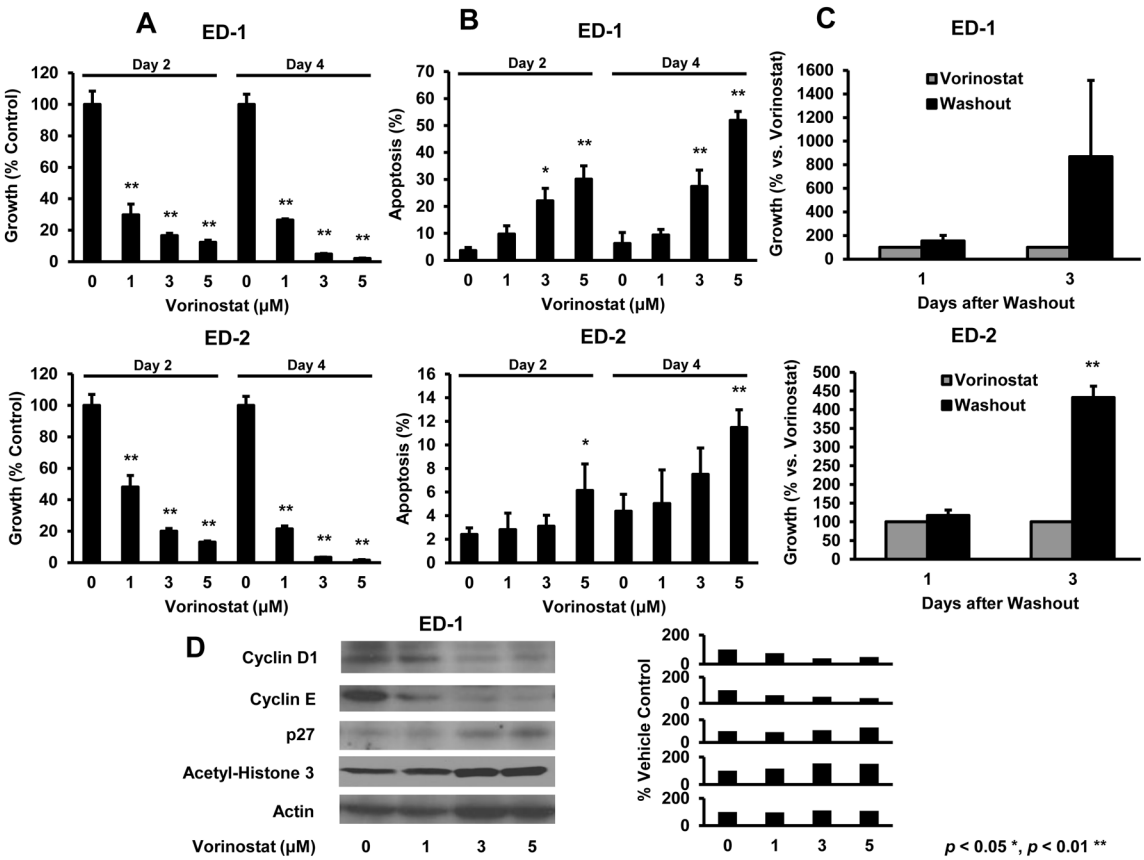

Fig. 1.

Vorinostat induced changes in proliferation, apoptosis and protein expression in murine transgenic lung cancer cell lines. Voinostat inhibited cell growth in a dose- and time-dependent manner in ED-1 (upper panel) and ED-2 (lower panel) cells versus controls and (B) also increased apoptosis in ED-1 (upper panel) and ED-2 (lower panel) cells versus vehicle controls. (C) Growth inhibition was antagonized in ED-1 (upper panel) and ED-2 (lower panel) cells by vorinostat washouts. (D) Vorinostat dose-dependent treatments decreased cyclin D1 and cyclin E protein, but increased p27 and acetyl-histone H3 levels in the representative ED-1 murine lung cancer cell line (signal intensity appears in the right panel). Symbols * and ** revealed significant changes $P < 0.05$ *and* $P < 0.01$, respectively.

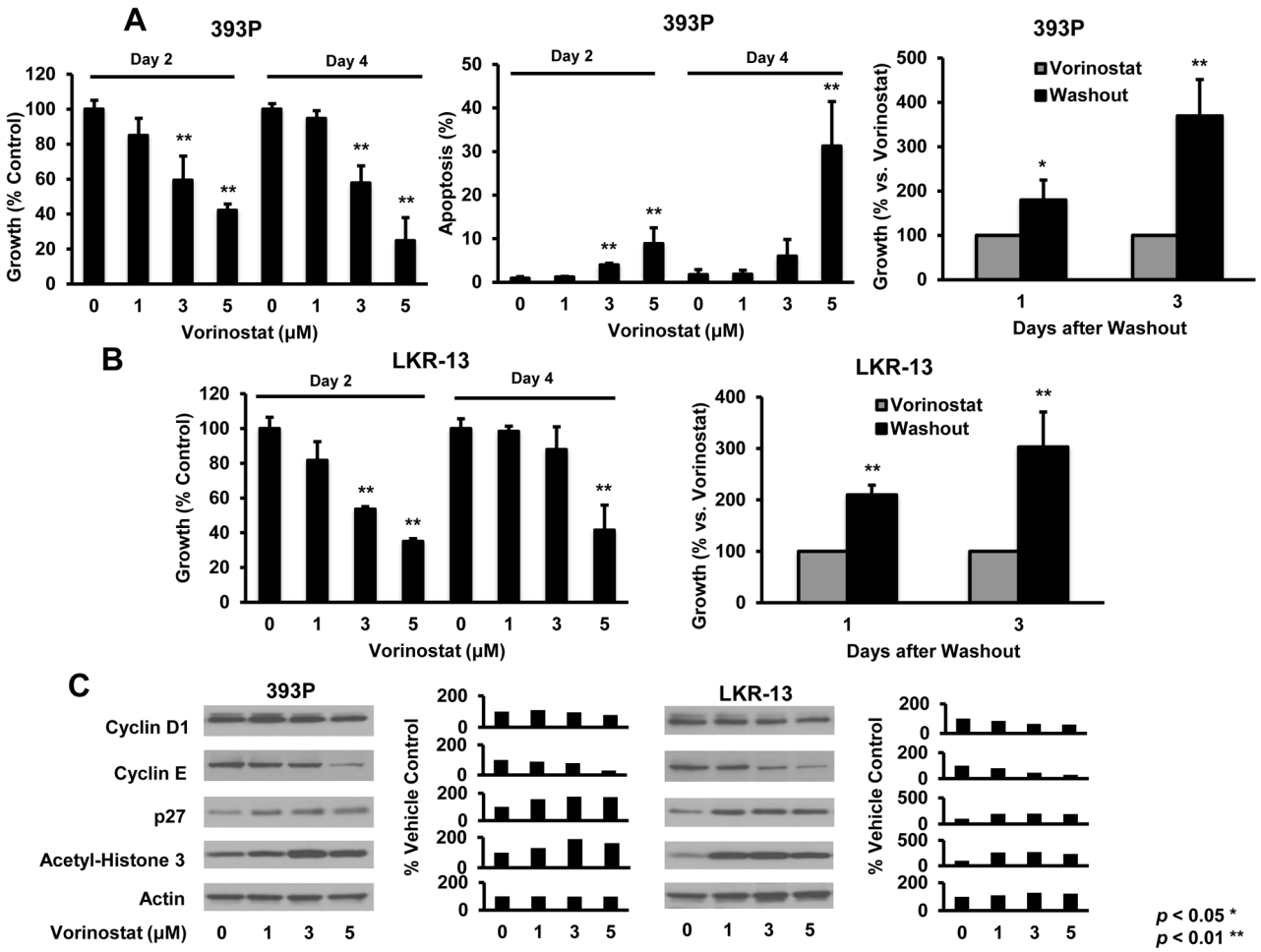

Fig. 2.

Vorinostat effects in murine 393P ($Kras^{LA1/+}$; $p53^{R172H\Delta G/+}$) and LKR-13 ($Kras^{LA2/WT}$) transgenic lung cancer cell lines. (A) Vorinostat inhibited growth in a dose-and time-dependent manner and increased apoptosis in 393P cells. Effects were antagonized by vorinostat washout. (B) Similar proliferation, apoptosis (data not shown) and washout effects occurred in LKR-13 cells. Vorinostat treatments decreased cyclin D1 and cyclin E proteins, but increased p27 and acetyl-histone H3 protein levels in 393P (left panel C) and LKR-13 (right panel C) cells. Respective signal intensities are quantified in the right panels). Symbols * and ** revealed significant *changes* $P < 0.05$ *and* $P < 0.01$, respectively.

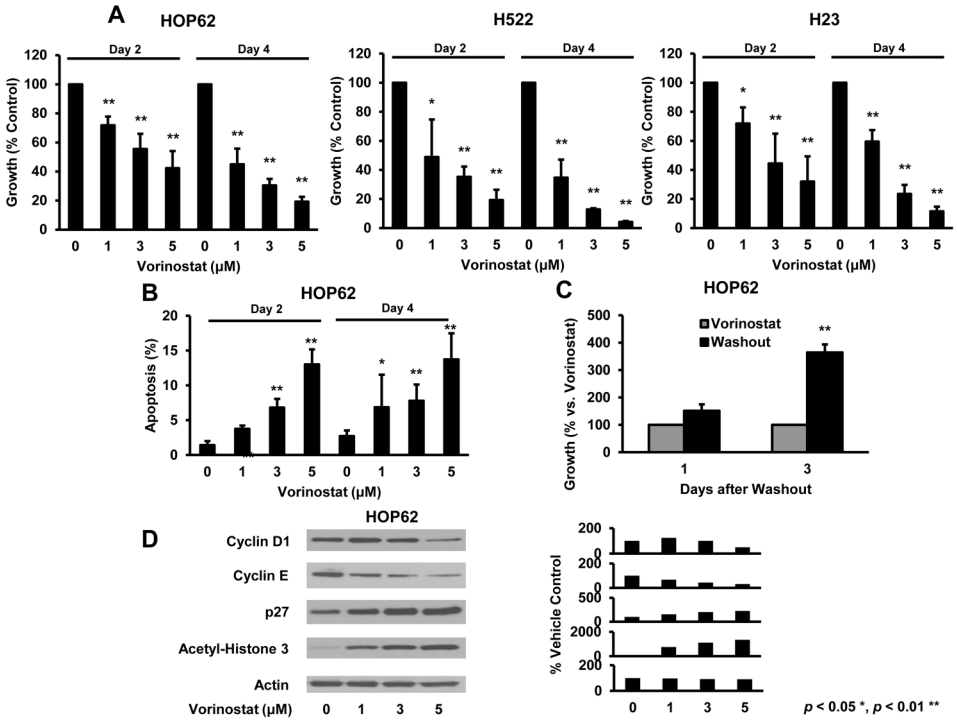

Fig. 3.

Vorinostat treatment effects in human lung cancer cell lines. (A) Vorinostat inhibited growth in a concentration- and time-dependent manner in HOP62 (left panel), H522 (middle panel) and H23 (right panel) human lung cancer cells versus vehicle controls. (B) Vorinostat induced apoptosis in a representative lung cancer cell line (HOP62). (C) Growth inhibition was antagonized by vorinostat washout of HOP62 cells. (D) Vorinostat induced similar dose-dependent changes in protein expression in human HOP62 versus murine lung cancer cell lines (Figs. 1 and 2). Signal intensity is shown in the right panel. Symbols * and ** revealed significant changes, $P < 0.05$ and $P < 0.01$, respectively.

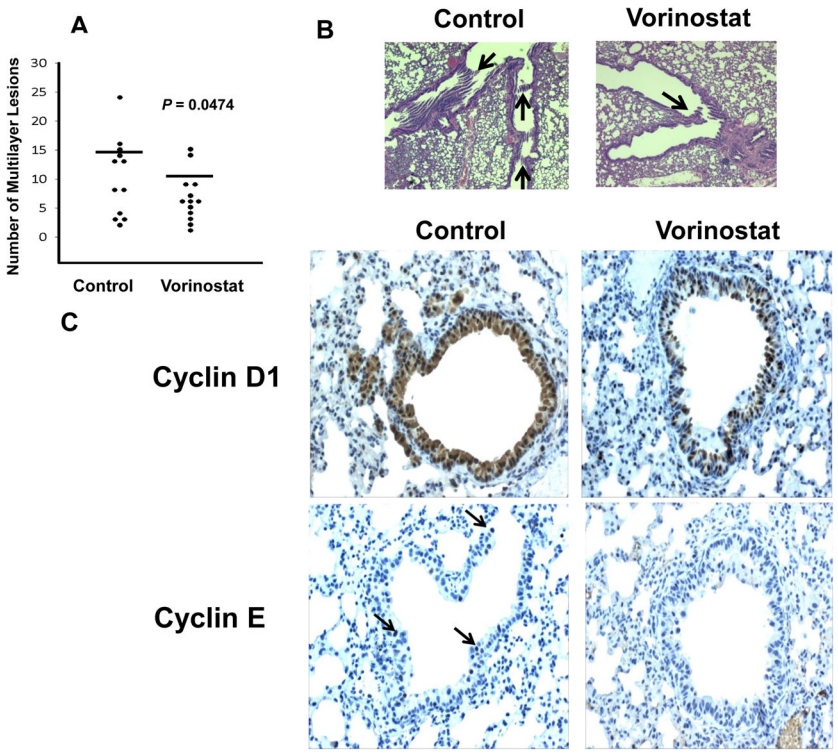

Fig. 4.

Vorinostat treatments of murine transgenic lung cancer models. (A) Vorinostat treatment reduced lung cancers in syngeneic tail-vein transplanted mice injected with ED-1 cells versus vehicle controls ($P = 0.047$). Each circle indicated a single mouse. The horizontal lines represented mean numbers of lung tumors. (B) Representative hematoxylin and eosin stained photomicrographs of malignant lung lesions (arrows) from syngeneic mice tail-vein injected with ED-1 cells followed by vehicle (control, left panel) or vorinostat (right panel) treatments. (C) Vorinostat versus vehicle-treated transgenic mice with lung cancers driven by human cyclin E. Vorinostat treatment (versus controls) reduced both cyclin D1 and human cyclin E (arrows) immunohistochemical expression. Immunostaining of representative lung tumors is shown (magnification x200).

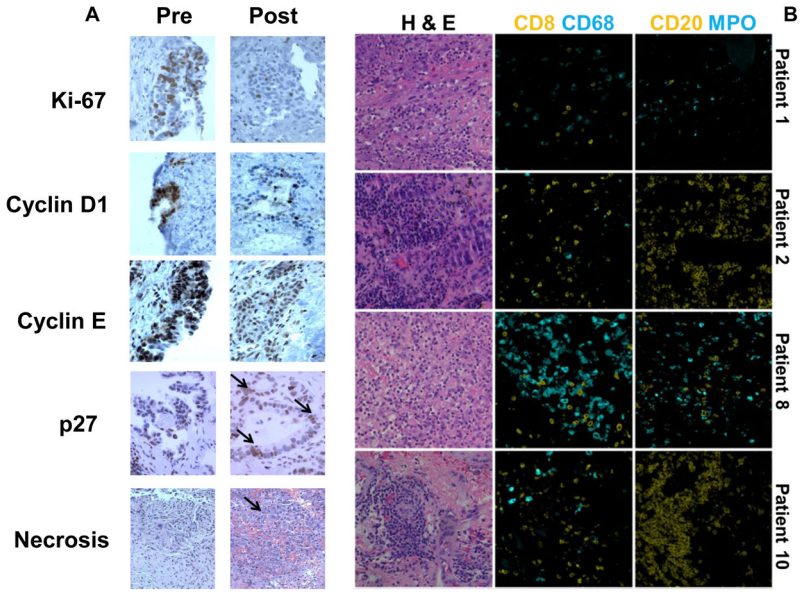

Fig. 5.

Pharmacodynamic effects in lung cancers treated in the vorinostat window of opportunity clinical trial. (A) Histopathologic and immunohistochemical profiles for Ki-67, cyclin D1, cyclin E, and p27 (arrow) in pre- versus post-vorinostat treatment from a representative lung cancer case (patient 3, 200X). Necrosis (arrow) was prominent in a representative post-treatment lung cancer (case 1,100X). (B) Post-vorinostat treatment, lung cancers exhibited marked inflammatory responses. Representative cases were used to detect immune cell subset-specific markers and hematoxylin and eosin (H & E) stained lung tumors after vorinostat treatment. Composite images and representative fields are displayed.

Table 1

Clinical, pharmacodynamic, pharmacokinetic and histopathologic responses of evaluable cases accrued to the vorinostat window of opportunity trial. Pharmacodynamic changes were post- versus pre-treatment.

Pt	Age/Sex/Smoker	Histology	Tx (days)	Serum ng/ml	Last dose (minutes)	Tumor ng/mg	Ki-67 %decrease	Cyclin E/D1 %decrease	K-ras	Necrosis increase	Acute/Chr Infl
1	59/F/Current	ADC	7	99.2	279	80.3	75	50/0	MUT	2+	3+/0
2	65/F/Former	ADC	7	28.0	366	42.8	67	73/0	WT	1+	1+/2+
3	64/F/Current	ADC	7	42.0	417	15.0	88	33/50	MUT	2+	2+/1+
4	71/M/Never	ADC/BAC	2	<LLQ	5 days	<LLQ	NA	NA	WT	0	0/2+
5	73/F/Former	ADC/BAC	7	36.0	295	46.9	0	ND/0	WT	0	0/1+
6	66/M/Current	SCC	3	<LLQ	4 days	<LLQ	ND	ND/0	WT	3+	3+/0
7	64/M/Current*	Eso-ADC	8	50.5	500	34024X	67	87/0	WT	0	0/0
8	69/M/Former	ADC	7**	7.3	178	<LLQ	42	0/↑	MUT	0	0/2+
9	70/M/Former	ADC/BAC	9	192.4	415	17.0	60	NA/↑	WT	0	0/0
10	69/M/Current	ADC	7	39.1	330	42.4	88	0/0	MUT	1+	0/1+

Symbols depicted

*esophageal cancer (Eso-ADC);

**100mg oral vorinostat daily treatment;

*X*replicate analysis confirmed this level, and ↑ for increased levels.

The lowest level of quantitation (LLQ) was 3ng/ml for serum and 12 ng/mg for cancers. Indicated abbreviations were: patient (Pt); treatment (Tx); male (M); female (F); not detected (ND); no cancer in the specimen (NA); KRAS codon 12 mutation (MUT); wild-type KRAS codon 12 (WT); adenocarcinoma (ADC); squamous cell carcinoma (SCC); bronchioloalveolar carcinoma (BAC); chronic (Chr) and inflammation (Infl).